



Recovery of silicon from metallurgical-grade silicon-refined slag by flotation with sodium silicate as depressant

Ning TAN¹, Shi-feng HAN¹, Dan-dan WU², Kui-xian WEI^{1,2}, Wen-hui MA^{1,2,3}

1. National Engineering Laboratory for Vacuum Metallurgy, Faculty of Metallurgical and Energy Engineering, Kunming University of Science and Technology, Kunming 650093, China;
2. State Key Laboratory of Complex Nonferrous Metal Resources Clean Utilization, Kunming University of Science and Technology, Kunming 650093, China;
3. Silicon Material Industry Research Institution (Innovation Center) of Yunnan Province, Kunming 650093, China

Received 6 December 2021; accepted 16 June 2022

Abstract: A flotation recovery method of silicon from metallurgical-grade silicon-refined slag (silicate) using sodium silicate (SS) as the depressant was proposed. The solution chemistry, contact angle, and zeta potential measurements were used to understand the interaction mechanisms of SS on the silicate. With SS addition, the content of recovered silicon increased from (72.12±5.08) wt.% to (81.14±1.77) wt.%. During the flotation process, SS was hydrolyzed into strongly hydrophilic H₂SiO₃ and HSiO₃⁻, which could be physically or chemically adsorbed with silicate. This adsorption allowed the contact angle of the silicate surface to decrease from 6.62° to 0°, indicating the decreasing floatability of the silicate.

Key words: metallurgical-grade silicon-refined slag; flotation; sodium silicate; depressant

1 Introduction

The global output of metallurgical-grade silicon (MG-Si) has steadily increased [1] due to its wide range of applications [2,3]. Metallurgical-grade silicon-refined slag (MGSRS), a solid waste, is produced during MG-Si refining and contains about 15 wt.% silicon [4,5]. This slag has not been effectively treated, resulting in a large loss of silicon resource and environmental problems. These challenges have become an increasing concern for MG-Si manufacturers [6–8]. The demand for the green and sustainable development of MG-Si must be met, and the comprehensive utilization of global resources has to be urgently developed. Effective measures need to be taken to recover silicon from MGSRS and use it in high-value applications [9,10].

In the study of the wet grinding process of MGSRS, TAN et al [11] found that silicon could be floated; thus, they proposed the possibility of recovering silicon by flotation process. In general, flotation can be used to effectively recover useful substances from solid wastes [12–15]. LARSEN and KLEIV [16] adopted hydrofluoric acid (HF) flotation to recover silicon from MGSRS. The surface of silicon was hydrophobic after HF treatment, allowing the enhanced recovery of silicon, and consequently, the separation of silicon and the silicate. Using flotation, LIU et al [17] determined that the recovered silicon powder (72.12% in purity) mainly contained elemental Si and low contents of Ca, Al, O, and C. Together with the silicon concentrate, some fine silicate particles were floated and adhered to the bubble during flotation. Thus, some silicate particles were entrapped in the recovered silicon particles, reducing

their purity. Therefore, to obtain higher-purity silicon, depressants should be used to modify the corresponding mineral surface performance [17–21] and inhibit the flotation of silicate minerals [22]. AZIZI and LARACHI [23] proposed the use of sodium silicate (SS) to inhibit the flotation of calcium-bearing silicate minerals and achieved good results.

SS can be used as a depressant to modify the surface of MGSRS and thereby improve the purity of recovered silicon. Meanwhile, silicon can be recovered from MGSRS via flotation. Therefore, in this work, the effects of SS addition on the purity of recovered silicon were investigated. The solution chemistry, contact angle, and zeta potential of SS were used to elucidate the interaction mechanisms between SS and silicate. Ultimately, an efficient flotation process for silicon recovery from MGSRS was developed.

2 Experimental

2.1 Materials and procedures

MGSRS and MG-Si were derived from the secondary refining process of MG-Si production in Yunnan Province, China. Silicon powder was collected by grinding MG-Si blocks to $\leq 74 \mu\text{m}$ particles. Analytically pure H_2SO_4 , Na_2CO_3 , and KCl were used in the experiments. The Na_2SiO_3 module was 2.31.

Figure 1 presents the experimental process of the MGSRS sample being crushed to particle with sizes $< 2 \text{ mm}$ to be used in flotation tests. Samples of about 300 g were fed into the rod mill, and 160 mL water was added for grinding. After the samples were ground for 15 min, the slurry of MGSRS was obtained. Flotation experiments were performed using an XFDIV flotation machine with a 1.0 L flotation cell. The impeller speed was set to 1992 r/min in the entire process of conditioning and flotation. After the samples were mechanically stirred for 1 min, reagents were added: a depressant (Na_2SiO_3), a frother, and a collector (terpenic oil) were sequentially added to the pulp. The dosages of SS were set to be 0, 100, 300, 500, and 700 g/t, successively. Silicon was then floated and absorbed onto the bubbles. For each test, the operating parameters were as follows: action time of 5 min for SS; action time of 1 min for terpenic oil; a scraping foam time of 10 min for the products. The

solution was filtered and dried at $60 \text{ }^\circ\text{C}$, and the recovered silicon was ultimately obtained.

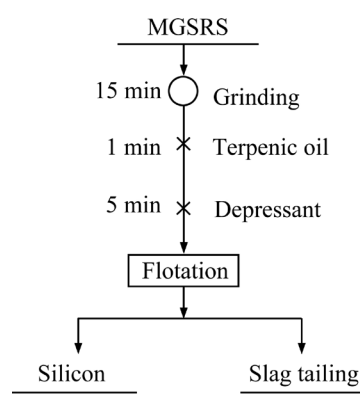


Fig. 1 Experimental flotation procedure

2.2 Analytical methods

The microstructures of the MGSRS samples were observed by scanning electron microscopy and energy-dispersive spectroscopy (SEM-EDS) (VEGA3 TESCAN). The silicon content in the samples was determined by two-step dissolution. The silicate was dissolved with 1–3 mL HCl for 1 g slag, and silicon was dissolved using a mixed acid solution of HNO_3 and HF with a volume ratio of 1:1. The pH value of the solution was measured using a pH meter (PHS-3C). A zeta potential analyzer (Malvern Zetasizer Nano-ZS90) was employed to determine the zeta potential of the samples. Before zeta potential testing, the raw material was ground in a three-head grinder to obtain powders finer than $2 \mu\text{m}$. A KCl solution with a concentration of 5 mmol/L was also prepared. When the desired dosage of SS was added to the KCl solution, the suspension was stirred for 1 min. After conditioning, the suspension was allowed to settle for 2 min, and the supernatant was added to the Malvin potential sample cells for testing. Each test was repeated 3 times, and the average was calculated. Solutions of 0.92 mol/L H_2SO_4 and 2 mol/L Na_2CO_3 were used to adjust the pH and the zeta potential of the MGSRS raw sample was measured. The contact angle of the powder samples was measured using a powder surface tensiometer (Krüss K100). In accordance with the Washburn equation [24] (Eq. (1)), the contact angle can be determined as follows:

$$m^2/t = \frac{Cp\varepsilon \cos\theta}{\eta} \quad (1)$$

where m is the mass gain, t is the flow time, C is the capillary constant, ρ is the liquid density, ε is the liquid surface tension, θ is the contact angle, and η is the liquid viscosity.

3 Results and discussion

3.1 Characterization of materials

3.1.1 Characterization of MGSRS

The microstructure and elemental composition of MGSRS, as visualized by SEM–EDS, are shown in Fig. 2.

As depicted in Fig. 2(a), MGSRS primarily contains silicon with apparent single silicon particles and a slag phase with numerous cracks. Figure 2(b) reveals clear interfaces between the silicon and slag, which facilitate the physical separation of silicon and slag. The elemental scanning results are shown in Fig. 2(c); MGSRS contains elements Si, Fe, Ti, Ca, Al, and O. This finding implies that the slag part consists of silicate particles. As the results suggest, some cracks of silicate particles are more easily broken, whereas most silicon particles are dense and difficult to

break. Silicon and silicate particles vary in breaking strength; with this difference considered, the preliminary separation of silicon and silicate particles by using physical methods is beneficial. The liberation of silicon and silicate particles is a prerequisite for the flotation process.

The electrical properties of the mineral surface are important factors affecting the selection and effect of the depressant, and thus are crucial in the flotation effect. Therefore, zeta potential analysis was conducted on the surface properties of the MGSRS raw sample, and the pH range varied from 3 to 11.

Figure 3 shows that when the pH is less than 6, the surface potential of MGSRS gradually approaches the point of zero charge (PZC). When the pH is 3.86, the potential of the system is -0.0757 mV, thus reaching PZC. Therefore, the PZC of MGSRS is 3.86. With an increase in pH, the potential value of the MGSRS surface gradually decreases [25]. This result indicates that the higher the alkalinity of the solution, the stronger the electronegativity of the MGSRS surface.

When the MGSRS powder was poured into the

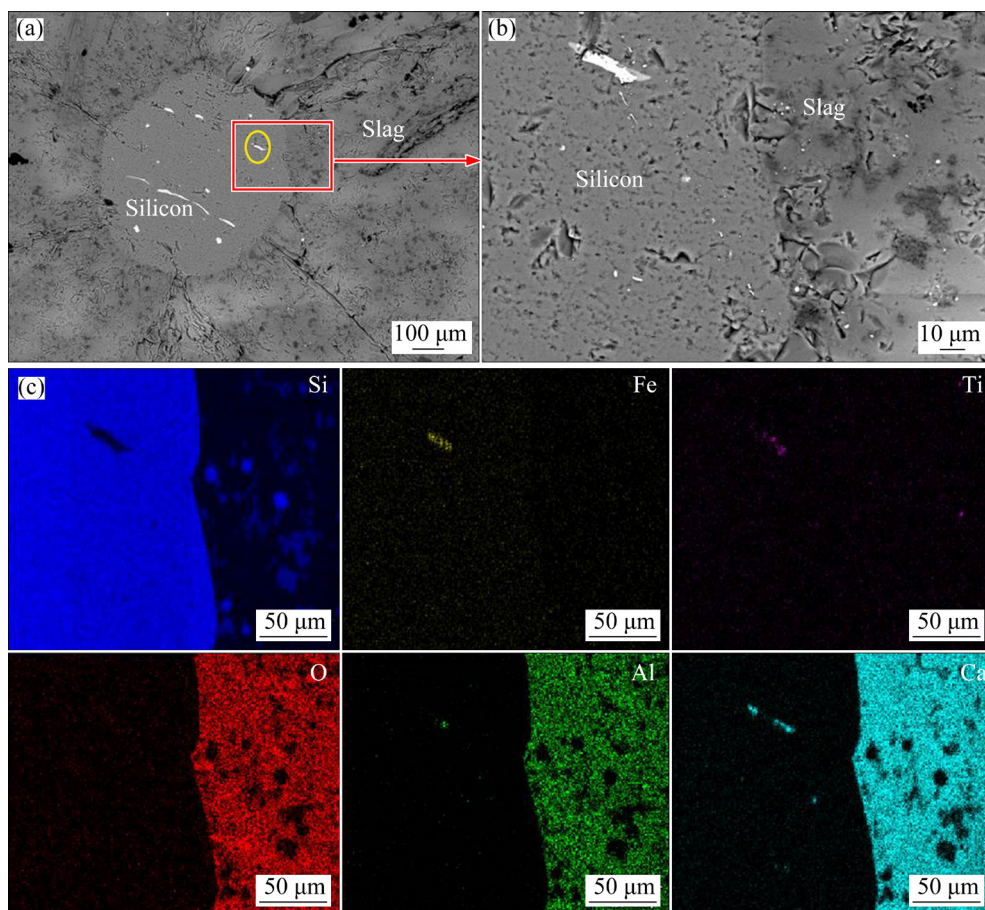


Fig. 2 Micromorphology (a, b) and elemental mapping analysis results (c) of MGSRS

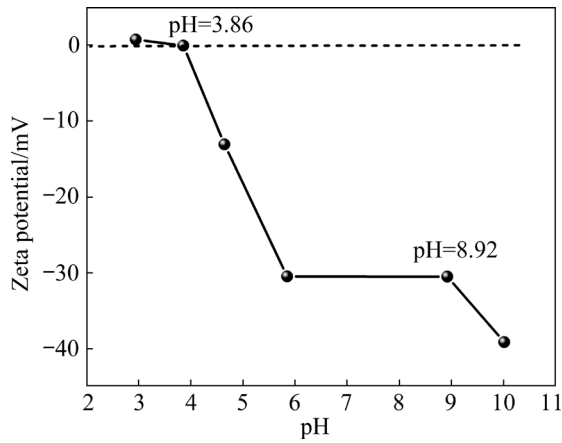
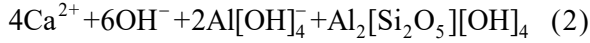
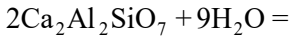


Fig. 3 Zeta potential of MGSRS under different pH conditions

KCl solution, the pH of the MGSRS raw sample reached 8.68, indicating alkalinity. The reason is that the MGSRS mainly consists of silicon and silicate particles, and the silicate is mostly composed of $\text{Ca}_2\text{Al}_2\text{SiO}_7$ (80%) [11]. In addition, hydrolytic reactions of silicate minerals can occur in an aqueous solution and provide hydroxide ions, as shown in Reactions (2) and (3):

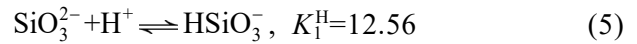
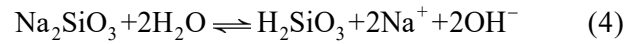


The hydrolysis of silicate minerals produces OH^- , which increases the pH of the pulp and causes the alkalinity increase of the solution. Simultaneously, Ca^{2+} , Al^{3+} , and other cation holes are generated on the silicate surface after hydrolysis [26]. SS is a common depressant of silicates in flotation. It can combine with cations on silicate surface because the silicate ions of SS are similar to those of silicates [27]. In addition, SS dissociated in water can produce polymers or colloidal particles with strong hydrophilicity. The hydrolysate of SS adsorbed on the surface of hydrophilic silicates improves its hydrophilicity, causing further depression of the silicate. Therefore, SS can be used to depress silicate.

3.1.2 Solution chemistry of SS

In flotation, the depressant dissociated in the aqueous solution can exist in different forms depending on the solution pH, which exerts important effects on flotation. SS is a strong alkali and weak acid salt. Several hydrolysis reactions can occur in the aqueous solution to form hydrolytic

products of various components. The reactions are shown in Reactions (4)–(6) [28]. Under different pH conditions, the direction of the hydrolysis and ionization reaction of SS can change, and the main components formed in the solution can also change. The proportion of each component of SS in the solution is calculated using solution chemistry to obtain the component concentrations of ions at different pH values. The specific calculation processes are shown in Eqs. (7)–(13):



$$K_1^{\text{H}} = \frac{[\text{HSiO}_3^-]}{[\text{SiO}_3^{2-}][\text{H}^+]} = 10^{12.56} \Rightarrow$$

$$[\text{HSiO}_3^-] = 10^{12.56} [\text{SiO}_3^{2-}][\text{H}^+] \quad (7)$$

$$K_2^{\text{H}} = \frac{[\text{H}_2\text{SiO}_3]}{[\text{HSiO}_3^-][\text{H}^+]} = 10^{9.43} \Rightarrow [\text{H}_2\text{SiO}_3] =$$

$$10^{9.43} [\text{HSiO}_3^-][\text{H}^+] = 10^{21.99} [\text{SiO}_3^{2-}][\text{H}^+]^2 \quad (8)$$

$$\beta_2^{\text{H}} = K_1^{\text{H}} \cdot K_2^{\text{H}} = 10^{12.56+9.43} = 10^{21.99} \quad (9)$$

$$[\text{Si}]_{\text{total}} = [\text{SiO}_3^{2-}] + [\text{HSiO}_3^-] + [\text{H}_2\text{SiO}_3] \quad (10)$$

$$\varphi_0 = \frac{[\text{SiO}_3^{2-}]}{[\text{Si}]_{\text{Total}}} = \frac{1}{1 + K_1^{\text{H}}[\text{H}^+] + \beta_2^{\text{H}}[\text{H}^+]^2} =$$

$$\frac{1}{1 + 10^{12.56}[\text{H}^+] + 10^{21.99}[\text{H}^+]^2} \quad (11)$$

$$\varphi_1 = \frac{[\text{HSiO}_3^-]}{[\text{Si}]_{\text{Total}}} = K_1^{\text{H}} \varphi_0 [\text{H}^+] = 10^{12.56} \varphi_0 [\text{H}^+] \quad (12)$$

$$\varphi_2 = \frac{[\text{H}_2\text{SiO}_3]}{[\text{Si}]_{\text{Total}}} = \beta_2^{\text{H}} \varphi_0 [\text{H}^+]^2 = 10^{21.99} \varphi_0 [\text{H}^+]^2 \quad (13)$$

Equations (9)–(13) indicate that the contents of different components in the hydrolyzed SS solution are only related to the pH value. On the basis of solution chemistry calculations, the species distribution of NaSiO_3 is depicted in Fig. 4.

Figure 4 presents the species distribution diagrams of SS as a function of pH. Three species (H_2SiO_3 , HSiO_3^- , and SiO_3^{2-}) are found in the SS solution. At $\text{pH} < 9$, the predominant silicate species is H_2SiO_3 [19], followed by HSiO_3^- ; at $\text{pH} = 9$, H_2SiO_3 and HSiO_3^- dominate the solution; at $9.4 < \text{pH} < 12.5$, HSiO_3^- is the main species [29]. At

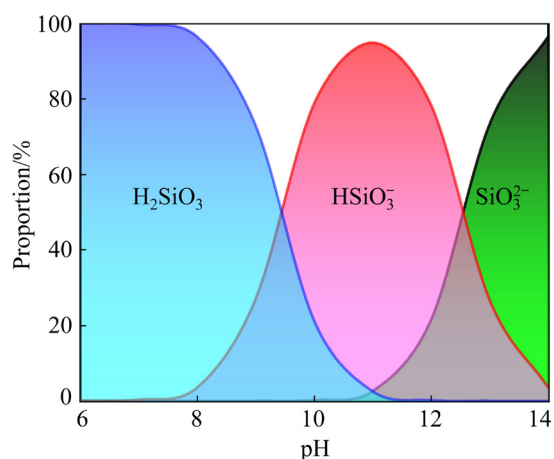


Fig. 4 Species distribution diagram of SS as function of pH

pH > 12.5, SiO_3^{2-} is the dominant species in the solution. However, strongly hydrophilic HSiO_3^- and H_2SiO_3 are the main depressant species of SS [30]. They are ideal depressants for the separation of metal and silicate minerals under low-alkali conditions. The aforementioned results indicate that under different pH levels, SS dominates the solution with different species, leading to different levels of inhibition. During flotation, the pH of the MGSRs pulp is 8.68. According to the results in Fig. 4, at $8 < \text{pH} < 10$, SS primarily exists as H_2SiO_3 and HSiO_3^- . Therefore, the H_2SiO_3 and HSiO_3^- dissociated from SS are selectively adsorbed on the silicate surface, enhancing the hydrophilicity of the silicate surface. Consequently, SS is shown to be an effective depressant on silicate minerals.

3.2 Effect of SS on content and contact angle of silicon and silicate

The effect of SS on the purity and recovery of silicon in flotation is illustrated in Fig. 5.

Figure 5(a) shows that the recovered silicon powder primarily contains Si and some Ca, Al, and O. Without SS addition, the contents of silicon and silicate recovered by flotation were $(72.12 \pm 5.08)\%$ and $(23.25 \pm 0.66)\%$, respectively. After SS addition, content of recovered silicon was $(81.14 \pm 1.77)\%$, reflecting an increase of 9.02% (Fig. 5(b)). Meanwhile, the content of silicate minerals was $(14.00 \pm 2.89)\%$, reflecting a decrease of 9.25%. These results indicate that the use of SS could significantly reduce the silicate content and improve the purity of the recovered silicon via flotation. SS addition led to the formation of

H_2SiO_3 and HSiO_3^- in the pulp, as indicated by the solution chemistry of SS, which are easily adsorbed on the silicate and improved the hydrophilicity of the silicate surface. Consequently, the hydrophilic differences on the surfaces of the silicon and silicate particles increased. Moreover, SS inhibited the flotation of silicate, benefiting the recycling of flotation for high-purity silicon.

The contact angle directly reflects changes in the wettability of material surfaces. It is an important technical indicator of the success of the flotation process [24]. In the current study, the flotation results indicate that SS significantly

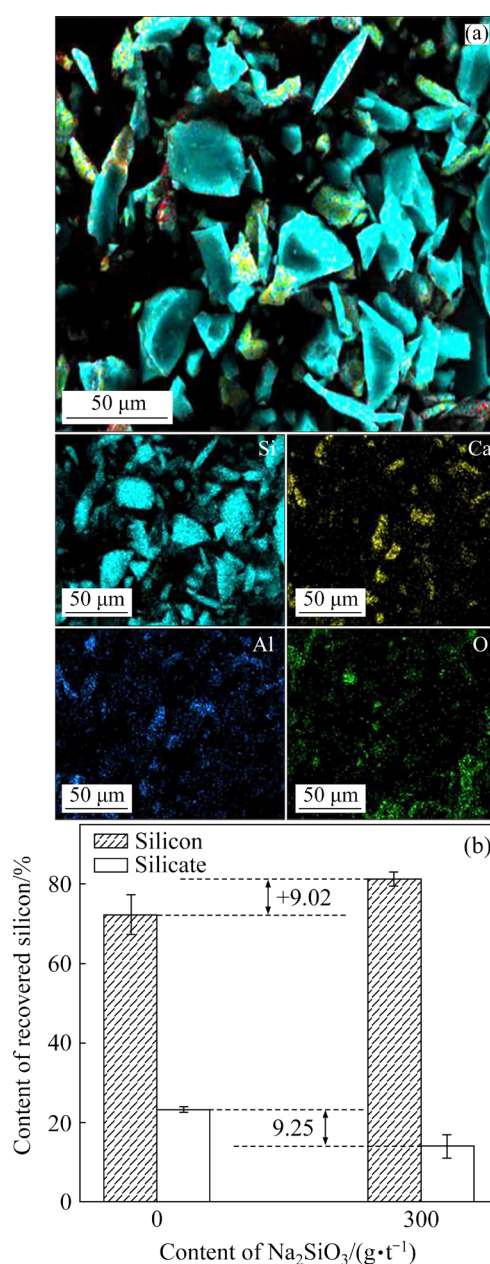


Fig. 5 Micromorphology (a) and content (b) of recovered silicon by flotation

inhibited the silicate. To further examine the inhibition mechanism of SS, the contact angles of silicon and silicates recovered from tailings were studied (Fig. 6).

Without SS, the adsorption constant C measured in the alcohol system was 0.5508271 mm^5 , and the fitting coefficient R^2 was 0.999735 ; the contact angle of the silicate tailings measured in the water system was 6.62° (Fig. 6(a)). The contact angle of the silicate tailings with SS addition decreased rapidly to 0° (Fig. 6(b)); the contact angle was zero when the surface of the silicate was totally hydroxylated [31]. These contact angle results indicate that SS addition caused an increase in the hydrophilicity of the silicate surface, strongly supporting the flotation results (Fig. 5) [32]. HSiO_3^- was easily produced by the hydrolysis of SS, and Ca^{2+} and Al^{3+} ions were chemically adsorbed on the silicate surface. H_2SiO_3 colloidal particles were also physically adsorbed on the silicate surface. Meanwhile, a hydrophilic hydration film was formed and wrapped on the silicate surface to enhance the hydrophilicity of the silicate surface. Further, the adsorption of terpene

oil on the silicate surface was inhibited. Finally, silicate particles as depressants settled to the bottom, further improving the purity of the recovered silicon. Figures 6(c) and (d) show that the contact angles of the recovered silicon surface have also changed. Without SS addition, the contact angle of the silicon recovered by flotation was 58.37° . After SS addition, the contact angle of the recovered silicon changed to 51.84° , reflecting a decrease of 6.53° . Owing to selective adsorption, SS could more easily adsorb on the silicate surface. However, with increasing SS content, the probability of SS adsorption on the silicon surface increased, and the contact angle decreased.

3.3 Effect of SS on pH and zeta potential of silicon and MGSRS

To investigate the mechanism of the effect of SS on flotation, changes in the pH of the solution and zeta potential after SS addition were further analyzed. These results are shown in Fig. 7.

The initial pH of the silicon solution system was 6.33 (Fig. 7(a)). With the increase in SS content, the pH of the solution increased to 6.47 ,

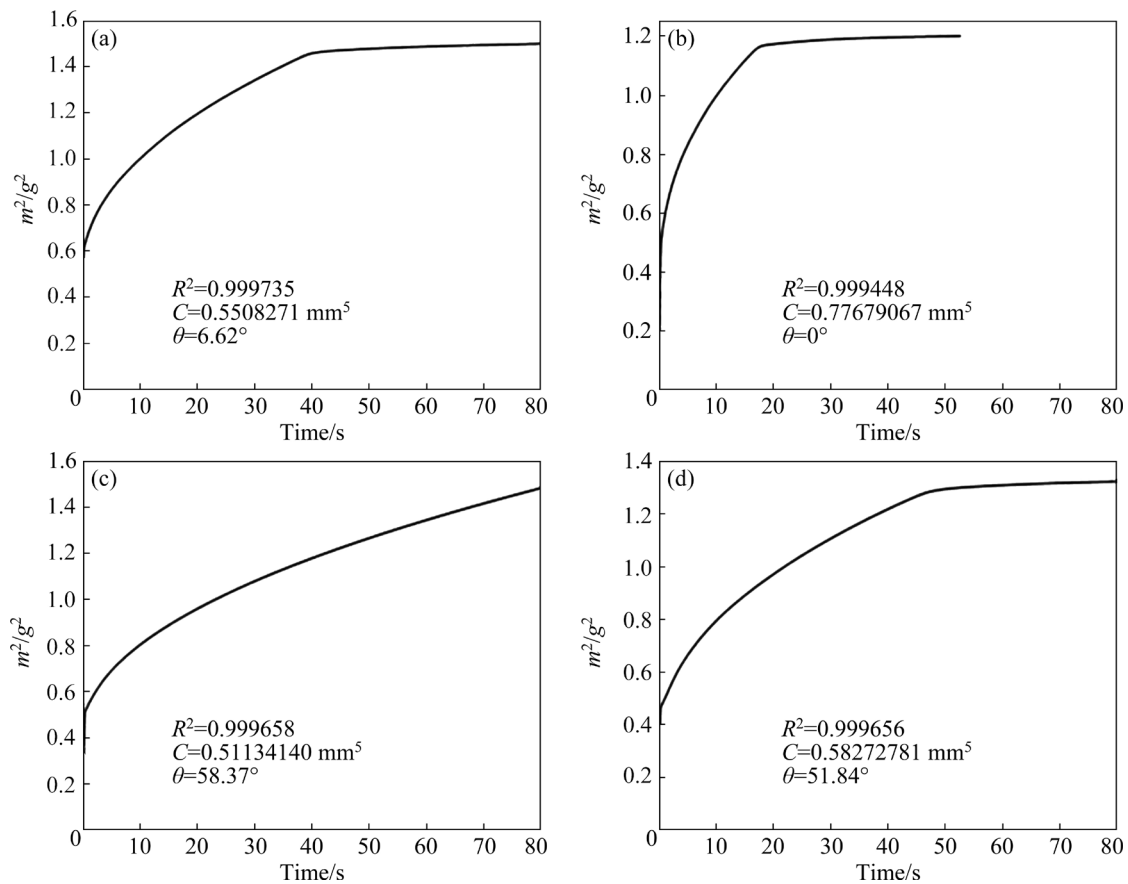


Fig. 6 Influence of SS on contact angle of sample surface: (a) Silicate tailings without SS; (b) Silicate tailings with SS; (c) Recovered silicon without SS; (d) Recovered silicon with SS

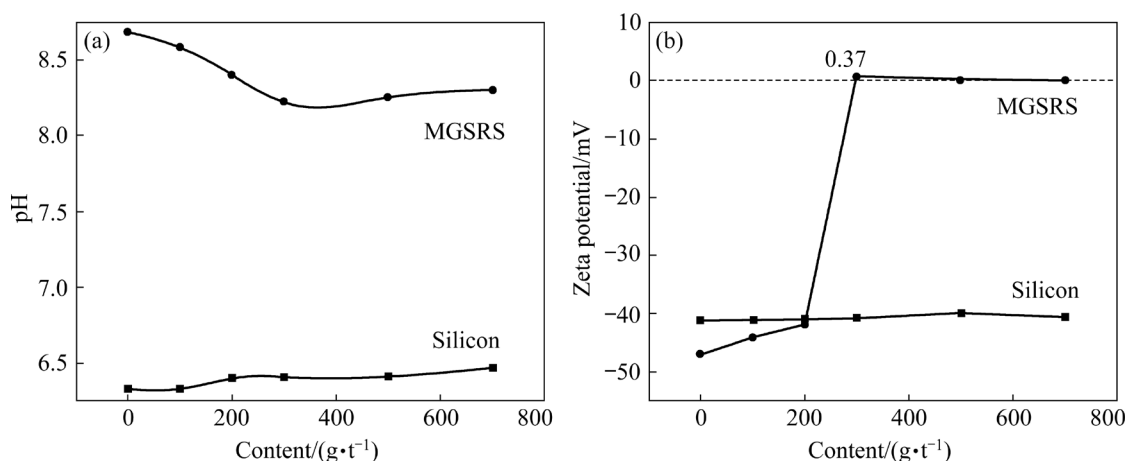


Fig. 7 Influence of SS content on pH (a) and zeta potential (b) of silicon slag and silicon systems

the maximum pH. OH^- ions could be generated by the dissociation of SS [33], increasing the solution pH. At pH levels of 6.33–6.47, the main species of SS were OH^- and H_2SiO_3 . Consequently, SS addition only slightly affected the pH of the silicon system. The initial pH of the MGSRS solution was 8.68. At this pH level, SS mainly existed as HSiO_3^- and H_2SiO_3 , which were selectively adsorbed onto the silicate surface. Meanwhile, OH^- ions in the solution combined with Ca^{2+} and Al^{3+} ions and then formed precipitates or slightly dissolved substances. Therefore, with a gradual increase in SS addition, the pH of the MGSRS solution system gradually decreased. Figure 7(b) shows the zeta potential results for MG-Si and MGSRS powder in the absence and presence of different contents of SS. With increasing contents of SS, the zeta potential of the MG-Si powder fluctuated within ± 2 mV. When the SS content was 300 g/t, the zeta potential was decreased by 0.37 mV. The aforementioned results showed that almost no adsorption occurred between SS and silicon at the initial stage of addition. With increasing SS content, only a small amount of SS was adsorbed on the silicon surface, leading to a decrease in potential. In the MGSRS system, SS addition is directly correlated with zeta potential. This relationship indicates SS adsorption on the silicate surface [23]. Owing to the adsorption of H_2SiO_3 and HSiO_3^- on the silicate surface, the zeta potential of the MGSRS system gradually increased with increasing SS content. When the content of SS reached 300 g/t, the pH of the MGSRS system was 8.22, and the zeta potential was close to its isoelectric point (PI). These results indicate that SS addition significantly affected

the zeta potential of MGSRS. As the hydrolysate of SS was adsorbed on the silicate surface and flocculated, the electrokinetic potential of the system approached PI, and the contact angle of the sample decreased (Fig. 6). This result agreed well with the flotation results. As silicates were added, the amount of silicate in recovered silicon decreased. In addition, as SS was adsorbed on the silicate surface, a more hydrophilic hydration film was formed. This film prevented the adsorption of terpenic oil on the silicate surface and promoted effective adsorption on the silicon surface. The results were conducive to improving the purity of recovered silicon.

3.4 Adsorption and depression mechanisms of SS on silicate

Based on the aforementioned experimental results, the action mechanism between SS and silicate minerals was investigated. The results are shown in Fig. 8.

Figure 8 shows the flotation process with terpenic oil as the collector, which has selectivity to silicon. The silicate surface also absorbed a certain amount of terpenic oil, resulting in entrapment and reducing the purity of recovered silicon. The addition of a depressant in the flotation process enhanced the hydrophilicity of the mineral surface by physical and chemical adsorption between the depressant and the mineral surface to inhibit the flotation of the silicate. The depressant SS was added first, followed by terpenic oil. The silicate surface with the adsorbed SS sank, and the silicon surface with adsorbed terpenic oil floated. With the selective inhibition of silicate by SS, silicon was

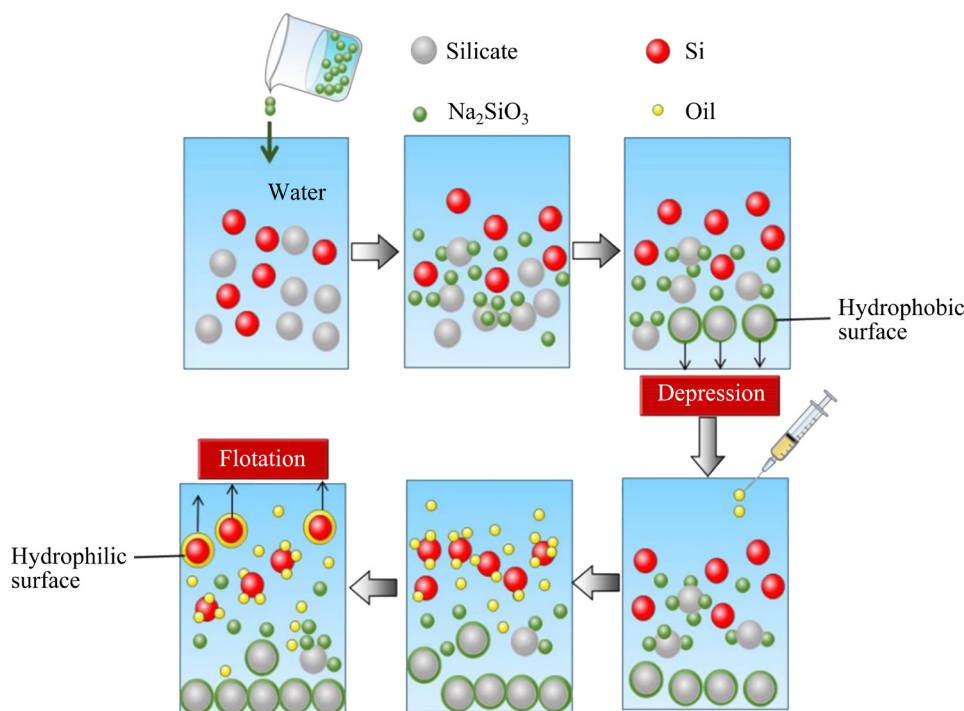


Fig. 8 Diagram showing mechanism of depressant effect of SS on silicate surface

separated from the silicate. The aforementioned experimental results show that SS can improve the hydrophilicity of silicate surfaces and significantly inhibit silicates in MGSRS. Solution chemistry calculations indicate that silicon products after SS hydrolysis exist in three forms: H_2SiO_3 , HSiO_3^- , and SiO_3^{2-} . The H_2SiO_3 and HSiO_3^- mainly exist in the form of colloid or polymer. QI et al [34] suggested that SS had a strong polymerizing effect on solution, and polymeric silicates or colloidal silicates were likely to exist in the form of selectively-inhibited flotation minerals. The polymerization degree of silicates depends on pH. At a certain pH, the tendency of polymeric species formation increases with rising sodium silicate content. As the polymer level increases, silicates change from a tetrahedral structure to a three-dimensional frame structure. In this study, the pH range is 8.22–8.68. Within this pH range, silicate primarily exists as H_2SiO_3 and HSiO_3^- , that is, the polymeric and colloidal states, respectively. Calcium and aluminum ions are found on the surface of the silicate after hydrolysis [35].

HSiO_3^- easily binds to positive ions on the silicate surface [36], and H_2SiO_3 exhibits strong hydrophilicity. The hydrophilic ends of each are adsorbed on the silicate surface and form a cladding layer. Therefore, polymer and silica gel with three-dimensional network structures are adsorbed

on the surface of the silicate. A tight hydrophilic layer is then formed, which can inhibit silicate flotation and prevent terpenic oil adsorption. Thus, the purity of the flotation-recovered silicon is improved. However, with increasing SS content, the solution pH gradually decreases. This effect can increase the chance of forming large silica colloidal particles or silica precipitation, thus reducing the adsorptive capacity of the silicate. Therefore, the increased content of SS does not necessarily lead to increased inhibitory effects. In addition, the precipitate consumed the activity of SS in the solution, further reducing the inhibitory effect. Therefore, at a certain pH level, the appropriate amount of SS efficiently inhibited silicate particles.

4 Conclusions

(1) The silicate phase in the MGSRS was dissociated in an aqueous solution, and the pH of the solution reached 8.68. Solution chemistry calculations indicate that when the pH was 8–9, SS was hydrolyzed and primarily existed as H_2SiO_3 and HSiO_3^- , significantly inhibiting the silicate minerals.

(2) When the pH of the MGSRS system reached 8.22, the contact angle of the silicate surface decreased from 6.62° to 0° , and the zeta

potential reached PI. When SS was added, the silicate content in the recovered silicon decreased by 9.25%, and the silicon content reached (81.14±1.77)%. The SS addition improved the hydrophilicity of the silicate surface, inhibiting the silicate and improving the recovered silicon purity.

Acknowledgments

This research was financially supported by the National Key R&D Program of China (Nos. 2018YFC1901805, 2018YFC1901801), the Reserve Talents of Young and Middle-aged Academic and Technical Leaders in Yunnan Province, China (No. 2018HB009), the Program for Innovative Research Team in University of the Ministry of Education of China (No. IRT-17R48), and the Major Project of Science and Technology Department of Yunnan Province, China (No. 2019ZE007).

References

- [1] HUANG Feng, CHEN Rui-run, GUO Jing-jie, DING Hong-sheng, SU Yan-qing. Removal of metal impurities in metallurgical grade silicon by cold crucible continuous melting and directional solidification [J]. *Separation and Purification Technology*, 2017, 188: 67–72.
- [2] XI Feng-shuo, LI Shao-yuan, MA Wen-hui, CHEN Zheng-jie, WEI Kui-xian, WU Ji-jun. A review of hydrometallurgy techniques for the removal of impurities from metallurgical-grade silicon [J]. *Hydrometallurgy*, 2021, 201: 105553.
- [3] MARTORANO M A, FERREIRA NETO J B, OLIVEIRA T S, TSUBAKI T O. Refining of metallurgical silicon by directional solidification [J]. *Materials Science and Engineering*, 2011, B176: 217–226.
- [4] HAN Shi-feng, TAN Ning, WEI Kui-xian, MA Wen-hui. Electromagnetic separation of silicon from metallurgical-grade silicon refined slag during the remelting process [J]. *Separation and Purification Technology*, 2022, 280: 119815.
- [5] WU Ji-jun, XU Min, MA Wen-hui, WANG Fan-mao, DAI Yong-nian. Research progress on boron removal from industrial silicon using gas blowing secondary refining technique [J]. *Journal of Kunming University of Science and Technology (Natural Science Edition)*, 2014, 39: 1–7. (in Chinese)
- [6] BJØRNSTAD E L, TRANELL G. Nucleation of SiO₂–CaO–Al₂O₃ slag in oxidative ladle refining of metallurgical grade silicon [J]. *Metallurgical and Materials Transactions B*, 2021, 52: 1392–1412.
- [7] ZHOU Qiang, WEN Jian-hua, WU Ji-jun. Recovery and purification of metallic silicon from waste silicon slag in electromagnetic induction furnace by slag refining method [J]. *Journal of Cleaner Production*, 2019, 229: 1335–1341.
- [8] QIAN Shuang-feng, CHEN Min. Experimental study on separation of silicon from industrial silicon slag [J]. *Nonferrous Metals Design*, 2017, 44: 18–22. (in Chinese)
- [9] JIANG Long-xiang, LU Jin-shan, CAO Jian-wei, WANG Zhi. Structure and properties of porous glass-ceramics sintered from metallurgical silicon slag [J]. *Transactions of Materials and Heat Treatment*, 2017, 38: 1–6. (in Chinese)
- [10] CAO Jian-wei, LU Jin-shan, JIANG Long-xiang, WANG Zhi. Oxidation behavior of metallurgical silicon slag under non-isothermal and isothermal conditions [J]. *Journal of Thermal Analysis and Calorimetry*, 2016, 124: 593–599.
- [11] TAN Ning, LI Hao, DING Zhao, WEI Kui-xian, MA Wen-hui, WU Dan-dan, HAN Shi-feng. Hydrogen generation during the purification of metallurgical-grade silicon [J]. *International Journal of Hydrogen Energy*, 2021, 46: 23406–23416.
- [12] LI Jing-wei, LIN Yin-he, SHI Jian, BAN Bo-yuan, SUN Ji-fei, MA Yong, WANG Fan-mao, LV Wei, CHEN Jian. Recovery of high purity Si from kerf-loss Si slurry waste by flotation method using PEA collector [J]. *Waste Management*, 2020, 115: 1–7.
- [13] LI H C, CHEN W S. Recovery of silicon carbide from waste silicon slurry by using flotation [J]. *Energy Procedia*, 2017, 136: 53–59.
- [14] ZHAO Chün-xiao, ZHONG Xue-hu. Reverse flotation process for the recovery of pyrolytic LiFePO₄ [J]. *Colloids and Surfaces A*, 2020, 596: 124741.
- [15] YAO Ya-Ke, ZHOU Kui, HE Jing-feng, ZHU Ling-tao, ZHAO Yue-min, BAI Qiang. Efficient recovery of valuable metals in the disposal of waste printed circuit boards via reverse flotation [J]. *Journal of Cleaner Production*, 2021, 284: 124805.
- [16] LARSEN E, KLEIV R A. Flotation of metallurgical grade silicon and silicon metal from slag by selective hydrogen fluoride-assisted flotation [J]. *Metallurgical and Materials Transactions B*, 2017, 48: 2859–2865.
- [17] LIU Cheng, SONG Shao-xian, LI Hong-qiang. Selective flotation of fluorite from barite using trisodium phosphate as a depressant [J]. *Minerals Engineering*, 2019, 134: 390–393.
- [18] JIAO Fen, DONG Liu-yang, QIN Wen-qing, LIU Wei, HU Chen-qiang. Flotation separation of scheelite from calcite using pectin as depressant [J]. *Minerals Engineering*, 2019, 136: 120–128.
- [19] GAO Yue-sheng, GAO Zhi-yong, SUN Wei, YIN Zhi-gang, WANG Jian-jun, HU Yue-hua. Adsorption of a novel reagent scheme on scheelite and calcite causing an effective flotation separation [J]. *Journal of Colloid and Interface Science*, 2018, 512: 39–46.
- [20] LAI Hao, DENG Jiu-shuai, FAN Gui-xia, XU Hong-xiang, CHEN Wen-xiang, LI Shi-mei, HUANG Ling-yun. Mechanism study of xanthate adsorption on sphalerite/marmatite surfaces by TOF-SIMS analysis and flotation [J]. *Minerals*, 2019, 9: 205.
- [21] BU Xian-zhong, FENG Yuan-yuan, XUE Ji-wei, YANG Lu, ZHANG Chong-hui. Effective recovery of chalcopyrite at low temperatures using modified ester collector [J]. *Transactions of Nonferrous Metals Society of China*, 2022, 32: 296–306.
- [22] VELOSO C H, FILIPPOV L O, FILIPPOVA I V, OUVRRARD S, ARAUJO A C. Investigation of the interaction mechanism of depressants in the reverse cationic

- flotation of complex iron ores [J]. Minerals Engineering, 2018, 125: 133–139.
- [23] AZIZI D, LARACHI F. Surface interactions and flotation behavior of calcite, dolomite and ankerite with alkyl hydroxamic acid bearing collector and sodium silicate [J]. Colloids and Surfaces A, 2018, 537: 126–138.
- [24] KARAGUZEL C, CAN M F, SONMEZ E, ÇELIK M S. Effect of electrolyte on surface free energy components of feldspar minerals using thin-layer wicking method [J]. Journal of Colloid and Interface Science, 2005, 285: 192–200.
- [25] UDAETA M C, PONOU J, DODBIBA G, FUJITA T. Enrichment of silicocarnotite from silicocarnotite and gehlenite mixtures using a kerosene-based liquid-liquid separation process [J]. Journal of Environmental Chemical Engineering, 2019, 7: 103387.
- [26] SUN Chuan-yao, YIN Wan-zhong. Silicate mineral flotation principle [M]. Beijing: Science Press, 2001. (in Chinese)
- [27] LIAN Xuan, PENG Zhi-hong, SHEN Lei-ting, QI Tian-gui, ZHOU Qiu-sheng, LI Xiao-bin, LIU Gui-hua. Properties of low-modulus sodium silicate solution in alkali system [J]. Transactions of Nonferrous Metals Society of China, 2021, 31: 3918–3928.
- [28] PARK C H, JEON H S. The effect of sodium silicate as pH modifier and depressant in the froth flotation of molybdenite ores [J]. Materials Transactions, 2010, 51: 1367–1369.
- [29] HUANG Li-huang. Flotation [M]. Beijing: Metallurgical Industry Press, 2018. (in Chinese)
- [30] ZHANG Zhui-guo, CAO Yi-jun, MA Zi-long, LIAO Yin-fei. Impact of calcium and gypsum on separation of scheelite from fluorite using sodium silicate as depressant [J]. Separation and Purification Technology, 2019, 215: 249–258.
- [31] GUNGOREN C, OZDEMIR O, WANG X, OZKAN S G, MILLER J D. Effect of ultrasound on bubble-particle interaction in quartz-amine flotation system [J]. Ultrasonics Sonochemistry, 2019, 52: 446–454.
- [32] JIN Sai-zhen, OU Le-ming, MA Xi-qi, ZHOU Hao, ZHANG Zheng-jun. Activation mechanisms of sodium silicate-inhibited fluorite in flotation under neutral and slightly alkaline conditions [J]. Minerals Engineering, 2021, 161: 106738.
- [33] WANG Yu-bin, WANG Yan, WEN Kan, DANG Wei-ben, XUN Jing-wen. Strengthening the inhibition effect of sodium silicate on muscovite by electrochemical modification [J]. Minerals Engineering, 2021, 161: 106731.
- [34] QI Gong-wen, KLAUBER C, WARREN L J. Mechanism of action of sodium silicate in the flotation of apatite from hematite [J]. International Journal of Mineral Processing, 1993, 39: 251–273.
- [35] MARINAKIS K I, SHERGOLD H L. Influence of sodium silicate addition on the adsorption of oleic acid by fluorite, calcite and barite [J]. International Journal of Mineral Processing, 1985, 14: 177–193.
- [36] ZHANG Wen-cai, HONAKER R Q. Flotation of monazite in the presence of calcite. Part II: Enhanced separation performance using sodium silicate and EDTA [J]. Minerals Engineering, 2018, 127: 318–328.

以硅酸钠为抑制剂浮选回收工业硅精炼渣中的单质硅

谭宁¹, 韩士锋¹, 吴丹丹², 魏奎先^{1,2}, 马文会^{1,2,3}

1. 昆明理工大学 冶金与能源工程学院 真空冶金国家工程实验室, 昆明 650093;
2. 昆明理工大学 复杂有色金属资源清洁利用国家重点实验室, 昆明 650093;
3. 云南省硅材料产业研究中心(创新中心), 昆明 650093

摘要: 提出一种以硅酸钠(SS)为抑制剂从工业硅精炼渣(硅酸盐)中浮选回收单质硅的新方法。通过溶液化学、接触角和 zeta 电位测试, 研究 SS 与硅酸盐的相互作用机理。研究发现, 添加 SS 后, 回收的硅含量从 (72.12±5.08)% (质量分数)提高至(81.14±1.77)% (质量分数)。浮选过程中, SS 水解成亲水性较强的 H₂SiO₃ 和 HSiO₃⁻, 与硅酸盐发生物理/化学吸附, 导致硅酸盐表面接触角从 6.62°降至 0°, 从而降低了硅酸盐的可浮性。

关键词: 工业硅精炼渣; 浮选; 硅酸钠; 抑制剂

(Edited by Wei-ping CHEN)